THE JOURNAL OF PHYSICAL CHEMISTRY B

Article

pubs.acs.org/JPCB

How Local and Average Particle Diffusivities of Inhomogeneous Fluids Depend on Microscopic Dynamics

Jonathan A. Bollinger, Avni Jain, and Thomas M. Truskett*

McKetta Department of Chemical Engineering, University of Texas at Austin, Austin, Texas 78712, United States

Supporting Information

ABSTRACT: Computer simulations and a stochastic Fokker–Planck equation based approach are used to compare the single-particle diffusion coefficients of equilibrium hard-sphere fluids exhibiting identical inhomogeneous static structure and governed by either Brownian (i.e., overdamped Langevin) or Newtonian microscopic dynamics. The physics of inhomogeneity is explored via the imposition of one-dimensional sinusoidal density profiles of different wavelengths and amplitudes. When imposed density variations are small in magnitude for distances on the scale of a particle diameter, bulk-like average correlations between local structure and mobility are observed. In contrast, when density variations are significant on that length scale, qualitatively different structure-mobility correlations emerge that are sensitive to the governing microscopic dynamics. Correspondingly, a previously proposed scaling between long-time diffusivities for bulk isotropic fluids of particles exhibiting Brownian versus Newtonian dynamics [Pond et al. *Soft Matter* **2011**, *7*, 9859–9862] cannot be generalized to describe the position-dependent behaviors of strongly inhomogeneous fluids. While average diffusivities in the inhomogeneous and homogeneous directions are coupled, their qualitative dependencies on inhomogeneity wavelength are sensitive to the details of the microscopic dynamics. Nonetheless, average diffusivities of the inhomogeneous fluids can be approximately predicted for either type of dynamics based on knowledge of bulk isotropic fluid behavior and how inhomogeneity modifies the distribution of available volume. Analogous predictions for average diffusivities of experimental, inhomogeneous colloidal dispersions (based on known bulk behavior) suggest that they will exhibit qualitatively different trends than those predicted by models governed by overdamped Langevin dynamics that do not account for hydrodynamic interactions.

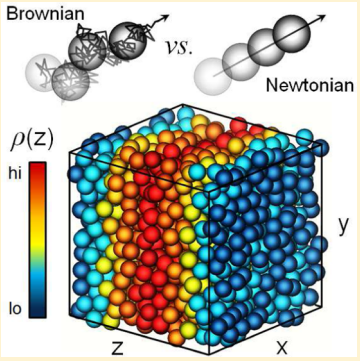

INTRODUCTION

Inhomogeneous fluids, which exhibit position-dependent structural (e.g., one-body density) and relaxation (e.g., diffusivity tensor) properties, are ubiquitous within natural and technological contexts due to the presence of external fields acting on their constituent particles or molecules. These external fields can originate from gravitational,[1−4] depletion,[5,6] electromagnetic,[7,8] and optical[9] forces, etc., which underlie phenomena including the sedimentation equilibrium of particle suspensions,[10] the strong positional ordering of fluids in contact with substrates,[11] and the precise entrapment of colloidal particles via optical tweezers,[12] as well as many other examples. While it is relatively well-understood how to predict the static structure of simple atomistic and colloidal fluids subjected to external fields,[13,14] fundamental microscopic theories that can anticipate corresponding dynamic responses within inhomogeneous fluids have only recently begun to emerge.[15−22] Since the interactions or external fields that induce fluid inhomogeneity can often be controlled experimentally, progress in relating inhomogeneous structure to dynamics is critical for the "inverse" design of new material systems with targeted transport properties.[23]

From a practical perspective, some of the most useful links between static and dynamic quantities are phenomenological structure–property correlations motivated by exact results for idealized systems.[24−27] Such correlations, which provide approximate connections between transport properties (e.g., shear viscosity and diffusivity) and static quantities (e.g., excess entropy), have aided in rationalizing and predicting the relaxation properties not only of dense bulk fluids with diverse interparticle potentials across a range of thermodynamic state points,[24−40] but also the dynamics associated with particle motions along isotropic directions of inhomogeneous fluids confined in various geometries (e.g., thin films, rectangular channels, or cylindrical pores).[41−50] Several recent investigations have also examined the position-dependent, single-particle diffusive dynamics that emerge within inhomogeneous fluids.[51−58] But because the calculation and interpretation of these position-dependent transport quantities are relatively new endeavors, little is known about the extent to which existing static-dynamic correlations for bulk fluids can be straightforwardly generalized to local particle motions in these systems.

In this work, we address a related question that, to our knowledge, has yet to be systematically explored: whether the local diffusive dynamics of inhomogeneous fluids are sensitive

Special Issue: Branka M. Ladanyi Festschrift

Received: September 2, 2014
Revised: October 27, 2014

   dx.doi.org/10.1021/jp508887r | J. Phys. Chem. B XXXX, XXX, XXX–XXX

to the type of microscopic dynamical rules governing the particle motions. Specifically, to what extent are qualitative trends in molecular transport dependent upon whether particles are governed by Brownian (i.e., stochastic) versus Newtonian (i.e., deterministic) physics? Addressing this question can provide new insights into which dynamic features, if any, can be expected to be universal across inhomogeneous fluids, thereby aiding in the development of theories for describing local relaxation processes and in the selection of appropriate simulation strategies for modeling their various behaviors. Regarding the latter point, pragmatic considerations often influence the selection of microscopic dynamics adopted in computer simulations of dense fluids; to wit, "coarse-grained" colloid trajectories are commonly generated with classical Newtonian dynamics, ignoring even the implicit effects of fast solvent degrees of freedom to improve computational efficiency.[59−62]

For bulk isotropic systems, it has been shown that these kinds of choices are justified: while short-time particle motions are sensitive to the type of microscopic dynamics, the long-time diffusion coefficients of equilibrium Brownian and Newtonian fluids are straightforwardly related for diverse interparticle potentials.[24−26,63−67] Likewise, the average relaxation properties of model glassformers are insensitive to the choice of microscopic dynamics (including Monte Carlo).[68−72] However, these findings deserve more careful scrutiny for other physical scenarios. For example, it remains unclear whether position-dependent diffusion coefficients of structurally identical inhomogeneous fluids computed independently from Brownian and Newtonian trajectories will relate to one another via the same semiempirical scaling laws observed in bulk isotropic fluids,[64,66] or whether they will even display the same qualitative trends for different strengths of density inhomogeneity.

To address whether the choice of microscopic dynamics qualitatively impacts mobility within inhomogeneous fluids, we build upon a previous study[57] in which we measured the single-particle long-time diffusivity coefficients of equilibrium hard-sphere fluids exhibiting periodic, one-dimensional (1D) sinusoidal density profiles from particle trajectories in the context of the 1D Fokker−Planck diffusion equation. Given that inhomogeneities can emerge at a variety of strengths and length scales depending on the nature the external field and the liquid constituents under consideration, we consider density profiles characterized by a variety of wavelengths and amplitudes. Though these periodically structured equilibrium fluids ought to be differentiated from more complex or nonequilibrium systems (e.g., specific multiphase interfaces, sheared fluids), they nonetheless capture some of the essential physics of inhomogeneity while remaining as simple as possible. Despite this simplicity, analogous correlations between local density and diffusivity have been observed in confined fluids and periodically structured fluids designed to imitate the structural characteristics of fluid interfaces.[52,57]

For pairs of inhomogeneous HS systems exhibiting identical static structures, which are simulated with Newtonian molecular dynamics (MD) and Brownian (i.e., overdamped Langevin) dynamics (BD), respectively, we compare position-dependent diffusivities $D_z(z)$ in the inhomogeneous direction and average diffusivities in all directions. For MD results, we draw upon (and augment) data from our previous publication, which considered only MD simulations.[57] We also examine local correlations between $D_z(z)$ and static quantities of interest for inhomogeneous HS fluids, including density $\rho(z)$, packing fraction $\phi(z)$, and the one-body direct correlation function $c^{(1)}(z)$, which characterizes local available volume.[73] We compare the accuracy of a simple phenomenological model[57] for predicting average diffusivities of BD and MD systems that draws upon knowledge of $c^{(1)}(z)$ and bulk fluid properties. We also assess the degree to which existing quantitative scalings between BD and MD long-time diffusivities in isotropic fluids[64,66] apply to local particle motions in inhomogeneous fluids.

As discussed below, we find that local and average diffusivity coefficients of strongly inhomogeneous fluids governed by BD and MD exhibit qualitative differences in terms of their correlations with static structure. Correspondingly, quantitative scalings between transport coefficients previously derived for bulk systems do not generally apply to local particle mobilities in these systems. However, we also show that average diffusion coefficients for inhomogeneous fluids subject to both types of microscopic dynamics can be approximately predicted via knowledge of the corresponding bulk isotropic fluid behaviors and the available volume distribution within the inhomogeneous fluids. Analogous predictions for average diffusivities of experimental colloidal dispersions with sinusoidal density profiles suggest, perhaps counterintuitively, that their qualitative behavior will more closely mimic the results of MD simulations than the BD simulations without hydrodynamics. This latter observation calls into question the utility of overdamped Langevin dynamics for capturing the physics of colloidal suspensions in strongly inhomogeneous states (e.g., under confinement).

COMPUTATIONAL METHODS

We examine systems of monodisperse hard-sphere (HS) particles modeled with the following continuous, steeply repulsive Weeks−Chandler−Andersen (WCA) pair potential:[74] $\varphi(r) = 4\varepsilon([\sigma/r]^{48} - [\sigma/r]^{24}) + \varepsilon$ for $r \leq 2^{1/24}\sigma$ and $\varphi(r) = 0$ for $r > 2^{1/24}\sigma$, where r is the interparticle separation. To simplify notation, we implicitly nondimensionalize quantities by appropriate combinations of the characteristic length scale σ and energy scale ε ($\varepsilon = k_BT$, where k_B is Boltzmann's constant and T is temperature).

To explore the effects of inhomogeneity length scale and magnitude, we consider equilibrium HS fluids exhibiting sinusoidal density profiles along the z-dimension, schematically illustrated in Figure 1. Local density $\rho(z)$ is defined by

$$\rho(z) = \rho_{avg} - (1/2)A\cos(2\pi z/\lambda) \quad (1)$$

where the average density is $\rho_{avg} = (2/\lambda)\int_0^{\lambda/2}\rho(z)dz$, A is the oscillation amplitude, and λ is the wavelength (similar to previous studies[75,76]). To impose the desired $\rho(z)$ profiles, we subject particles to one-body external potentials $\varphi^{osc}(z)$ that are analytically calculated via Fundamental Measure Theory (FMT),[14] which has been shown to accurately describe the structural and thermodynamic properties of inhomogeneous HS fluids for the densities considered here.[14,45] Note that in the absence of the external fields, the fluid regions under consideration would simply exhibit bulk properties corresponding to ρ_{avg}.

Beyond local density $\rho(z)$, we also consider two structural properties that are well-defined for the HS fluid and encode greater information about particle packing: the local packing fraction $\phi(z)$ and the one-body direct correlation function

dx.doi.org/10.1021/jp508887r | J. Phys. Chem. B XXXX, XXX, XXX−XXX

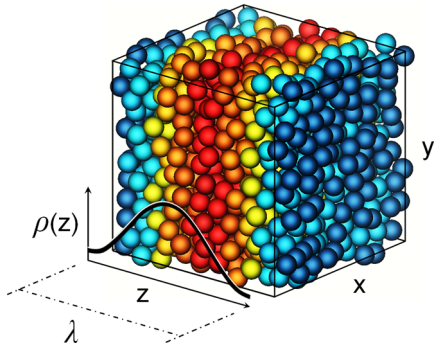

Figure 1. Schematic of the inhomogeneous fluids under consideration. Systems consist of equilibrium HS fluids exhibiting 1D sinusoidal density profiles $\rho(z)$ of wavelength λ (see eq 1) due to the imposition of z-dependent external fields. Particles are shaded based on their instantaneous location within low-density (blue) vs high-density (red) regions.

$c^{(1)}(z)$. Local packing fraction $\phi(z)$ is straightforwardly obtained from $\rho(z)$ via

$$\varphi(z) = \pi \int_{z-1/2}^{z+1/2} \rho(z')\left(\frac{1}{4} - (z' - z)^2\right)\mathrm{d}z' \tag{2}$$

and quantifies the average areal fraction of the plane located at z that is occupied by particle cores. The quantity $c^{(1)}(z)$ is obtained from FMT, where $c^{(1)}(z) = \ln p_0(z)$ and $p_0(z)$ is the average areal fraction of the plane located at z that can accommodate insertion of an additional hard-sphere center without overlap with existing particles.[73] In essence, $c^{(1)}(z)$ quantifies the distribution of local "available space" in the system. In the bulk isotropic fluid, $p_0 = \exp\{c^{(1)}\} = \exp\{-\mu^{ex}\}$ and quantifies the particle insertion probability, where μ^{ex} is the excess chemical potential (relative to an ideal gas at the same density).

In terms of particle dynamics, diffusion provides an excellent description of motions over times t much greater than the intervals between particle collisions. For isotropic systems of dimensionality d where particles experience zero net force, the Einstein equation, $\langle \Delta \mathbf{r}^2 \rangle = 2dDt$, relates the diffusion coefficient D to the mean-squared displacement $\Delta \mathbf{r}^2$. However, to describe particle displacements along inhomogeneous dimensions of varying density, the Einstein relation is no longer appropriate because diffusion coefficients are spatially varying and particles experience nonzero average net forces.[51] For fluids exhibiting 1D inhomogeneity along a coordinate z, it has instead been shown[52] that particle displacements follow the 1D Fokker–Planck (FP) equation

$$\frac{\partial G}{\partial t} = \frac{\partial}{\partial z}\left(D_z(z)\mathrm{e}^{-F(z)}\frac{\partial}{\partial z}[e^{F(z)}G]\right) \tag{3}$$

with position-dependent diffusion coefficients $D_z(z)$. Here, $G(z,t_0 + \Delta t|z',t_0)$ is the Markovian propagator describing temporal single-particle displacements given a nonuniform potential of mean force $F(z) = -\ln\{\rho(z)\} + C$, where C is an arbitrary constant.

In this study, we specifically consider the steady-state (i.e., $\partial G/\partial t = 0$) limit of the FP equation, and use a previously published mean-first passage times (MFPT) method[77,78] to derive $D_z(z)$ coefficients via

$$D_z(z) = -\frac{\exp\{F(z)\}}{\partial \tau(z, z_t)/\partial z}\int_{z_{refl}}^{z} \exp\{-F(z')\}\mathrm{d}z' \tag{4}$$

This expression assumes a reflective (i.e., nonperiodic) boundary at z_{refl} and an absorbing boundary at $z_t > z_{refl}$, where $\tau(z, z_t)$ is the ensemble-averaged MFPT of particles starting from $z_{refl} < z < z_t$ at $t = t_0$ and crossing $z = z_t$ at $t = t_0 + \tau(z,z_t)$. We filter the MFPT information to exclude short-time non-Markovian displacements, which are straightforward to identify,[53,78] and subsequently obtain quantitative coefficients of diffusive (as opposed to ballistic) motion through different regions of the fluid. We have tested to ensure that the MFPT method agrees with $D_z(z)$ coefficients obtained from a Bayesian analysis of the FP equation[52] using z displacement data from simulations. We have also tested that it yields results in agreement with a color counterdiffusion steady-state solution of the FP equation.[58]

The MFPT analysis requires nonperiodic boundary conditions in the z-dimension, so we generate suitable trajectories from simulations subject to external potentials that stitch together the FMT-derived $\varphi^{osc}(z)$ fields and purely repulsive confining potentials. The confining walls are separated by distances large enough (i.e., there is enough buffer volume) to ensure that the static and dynamic properties in the "core" regions of interest with oscillatory profiles are unaffected by the external confinement, which is straightforward to verify in these systems. Because calculating $D_z(z)$ coefficients requires extensive trajectory data, we perform these MD and BD simulations using GROMACS 4.5.5[79] to facilitate parallelization.

We note one important modification to the MFPT approach as originally presented:[53,78] when analyzing the MD trajectories, we do not track all particles located at $z < z_t$ at time t_0, but instead track only a fraction of them with probability p. We employ this change based on previous studies using the MFPT method and related approaches for ballistic HS,[57,58] where it was found that by tracking all particles (i.e., $p = 1.0$), the velocity distributions of "tagged" particles near the reflective boundaries are incorrectly biased toward faster particles relative to the appropriate Maxwell–Boltzmann distribution. This, in turn, results in artificially elevated diffusivities near the reflective boundaries (particularly if extended low-density regions are situated nearby), because an insufficient number of collisions have occurred to redistribute particles' momenta. We find that $p \leq 0.01$ is sufficient to eliminate bias in all of our systems, and as $\lambda \to 1$, we find the bias can be corrected by less selective probabilities $p \leq 0.2$. Thus, we choose $p = 0.01$ for wavelengths $\lambda \geq 12$ and $p = 0.05$ for $1 \leq \lambda \leq 6$, since increasing p lessens that amount of trajectory information required to obtain smooth diffusivity profiles. For the BD trajectories, however, this selectivity is unnecessary because inertia is ignored; thus, $D_z^{BD}(z)$ profiles are unaffected by the choice of p.

Diffusion coefficients in the homogeneous direction, D_{xy}, are obtained from separate simulations performed with a custom program in which periodic boundary conditions are applied in all three dimensions, with box lengths in the z-direction being multiples of λ. D_{xy} values are extracted by fitting the long-time ($t \gg 1$) behavior of the average mean-squared displacement to the Einstein relation $\langle \Delta \mathbf{r}^2 \rangle = 4D_{xy}t$, where $\Delta \mathbf{r}^2$ represents the mean-squared displacement of each particle in the x and y directions.

BD trajectories are generated by solving the overdamped Langevin equation in the absence of hydrodynamic interactions

dx.doi.org/10.1021/jp508887r | J. Phys. Chem. B XXXX, XXX, XXX–XXX

for systems of $N = 2400$ particles. The position $\mathbf{r}_i$ of each particle $i \in [1,N]$ at time t is updated with time-step $\Delta t = 0.02$ according to the following expression:[80,81]

$$\mathbf{r}_i(t + \Delta t) = \mathbf{r}_i(t) + D_0 \Delta t \mathbf{F}_i(\mathbf{r}_i(t)) + \boldsymbol{\xi}_i(t) \quad (5)$$

where $D_0 = 0.001$ is the infinite dilution ($\rho \to 0$) diffusivity, $\mathbf{F}_i(t)$ is the force on each particle due to interparticle and external potential interactions, and $\boldsymbol{\xi}_i(t)$ is the stochastic contribution to motion. In each dimension, $\xi_i(t) = r_i^G(t)\text{-}(2D_0\Delta t)^{1/2}$, where $r_i^G(t)$ is a Gaussian distributed white noise with $\langle r_i^G(t)\rangle = 0$ and standard deviation $\sigma = 1$. MD simulations are identical to the BD simulations with respect to population ($N = 2400$), structure, and thermodynamics, and detailed simulation protocols are included in our previously published study.[57]

RESULTS AND DISCUSSION

Local Dynamics of Inhomogeneous Fluids. We begin by discussing Figure 2, which shows how local density $\rho(z)$ relates to local diffusivity in the inhomogeneous z-direction $D_z(z)$. The latter is calculated from BD $[D_z^{BD}(z)$, normalized by $D_0]$ and MD $[D_z^{MD}(z)]$ simulations for several wavelengths λ. The BD and MD systems at each λ are identical in terms of their inhomogeneous static structures, which isolates the effect of microscopic dynamics on local single-particle mobility. Note that BD data and MD data are plotted on linear and logarithmic axes, respectively. This is done because of the much larger diffusivity range in MD (up to an order of magnitude) and to facilitate comparisons with past studies.[57,64] This treatment is applied through the remainder of this section.

To simplify the analysis, we fix the average density ρ_{avg} and the amplitude A defining $\rho(z)$ such that we consider only structural variations with respect to inhomogeneity wavelength λ. We choose $\rho_{avg} = 0.573$, which corresponds to a moderately dense bulk HS fluid (the freezing density of the isotropic fluid occurs at $\rho_f^{bulk} = 0.943$). The density range $\rho(z) = [0.287,0.860]$ encompasses nearly two-thirds of the bulk HS fluid regime, across which mean bulk collision frequencies vary by approximately an order of magnitude. For these density ranges, the potential depths of $\varphi^{osc}(z)$ range from $|\varphi_{max}^{osc}(z) - \varphi_{min}^{osc}(z)| < 1$ for $\lambda = 1.0$ up to $|\varphi_{max}^{osc}(z) - \varphi_{min}^{osc}(z)| \approx 12$ when $\lambda = 24$ (see Figure S1 in the Supporting Information).

For the longer wavelengths in Figure 2 (e.g., $\lambda \geq 6$), both $D_z^{BD}(z)$ and $D_z^{MD}(z)$ are negatively correlated with local density, meaning that mobility is slowed through more highly packed regions. This is intuitively expected based on the physics of the bulk HS fluid, which exhibits a negative correlation between self-diffusivity and density. However, as the inhomogeneity wavelength decreases to $\lambda \leq 3$, correlations between local density and diffusivity exhibit intriguing sensitivities to both wavelength λ and the type of microscopic dynamics. First consider $\lambda = 2.5$, where $D_z^{BD}(z)$ exhibits negative correlations with $\rho(z)$ (not unlike those at larger λ), while $D_z^{MD}(z)$ becomes virtually insensitive to the strong variations in local density, the latter a remarkable behavior we noted previously.[57] Even more interesting and distinct behaviors emerge between $2.5 \geq \lambda \geq 1.0$. Here, the BD systems exhibit two sequential crossovers in terms of the correlations between $D_z^{BD}(z)$ and $\rho(z)$, from negative at $\lambda = 2.5$ to positive at $\lambda = 1.2$ and back to negative at $\lambda = 1.0$. Meanwhile, in the MD systems, there emerges a growing positive correlation between $D_z^{MD}(z)$ and $\rho(z)$ that is most prominent around $\lambda = 1.2$ to 1.0, an observation made in other MD studies[52,55] of highly confined fluids exhibiting density profiles of $\lambda \simeq 1$.

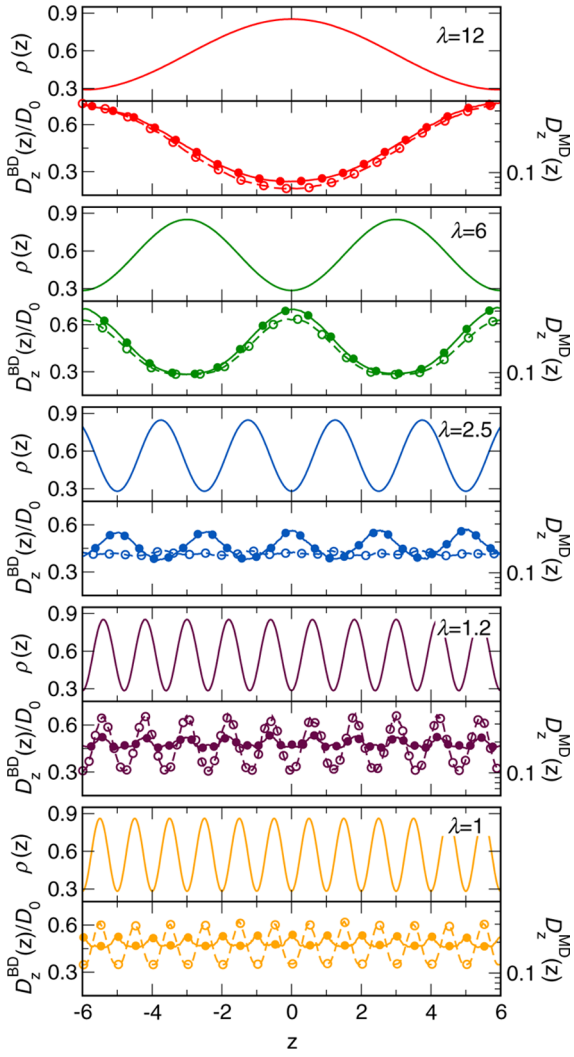

Figure 2. Position-dependent density $\rho(z)$ and diffusivities in the inhomogeneous z-direction $D_z^{BD}(z)$ (closed symbols, left y-axis) and $D_z^{MD}(z)$ (open symbols, right y-axis), calculated from BD and MD simulations, respectively, of HS fluids exhibiting sinusoidal density profiles with $\rho_{avg} = 0.573$, $\rho(z) = [0.287,0.860]$, and wavelengths $\lambda = 12$, 6, 2.5, 1.2, and 1.0. Error bars are on the order of the scale of the symbols. MD data are from a previous study by the authors.[57]

Altogether, local diffusivities from both BD and MD are qualitatively similar for sufficiently long λ, where they display behaviors that appear to be simple extensions of bulk-fluid like physics. But nontrivial static-dynamic correlations specific to BD or MD emerge as λ decreases below several particle diameters, not only highlighting that intuitions about local behaviors should not be naïvely extrapolated from bulk fluids, but also offering evidence that the expected qualitative connections between position-dependent mobilities of systems governed by different microscopic dynamics do not hold in strongly inhomogeneous states.

The comparisons in Figure 2 are recast and augmented in the left panel of Figure 3, which directly compares local diffusivity versus density for BD (main) and MD (inset) over an expanded collection of λ values. Here, the transition from negative correlations at large λ to the breakdown of bulk-like behaviors at small λ is evident, demonstrating that $\rho(z)$ does

dx.doi.org/10.1021/jp508887r | J. Phys. Chem. B XXXX, XXX, XXX−XXX

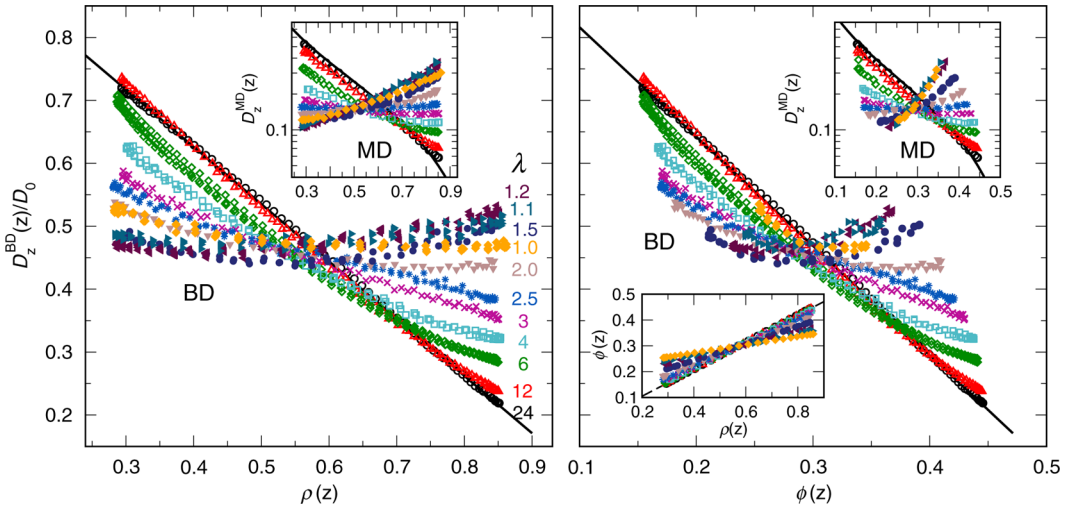

Figure 3. Position-dependent diffusivities in the inhomogeneous z-direction $D_z^{BD}(z)$ and $D_z^{MD}(z)$ (insets) plotted vs local density $\rho(z)$ (left panel) and local packing fraction $\phi(z)$ (right panel) for HS systems at $\rho_{avg} = 0.573$, $\rho(z) = [0.287,0.860]$, and $\lambda = 24$ (black), 12, 6, 4, 3, 2.5, 2.0, 1.5, 1.2, 1.1, and 1.0 (gold). Error bars are on the order of the scale of the symbols. Data for the bulk HS fluid are shown as solid black lines. Bottom inset in right panel illustrates the linear relationships between $\phi(z)$ and $\rho(z)$ at all wavelengths. MD data are from a previous study by the authors.[57]

not exhibit any "universal" relationship with local particle mobility in strongly inhomogeneous fluids. For $\lambda \geq 12$, the curves for BD and MD are virtually indistinguishable from the respective D_ρ^{bulk} versus ρ curves, indicating that for sufficiently gradual density variations, particles experience a continuum of bulk-like regions with respect to local mobility. Of course, this must be true as $\lambda \to \infty$ for the finite A considered here, but it is notable that even for such large amplitudes of $\rho(z)$, the characteristic inhomogeneity length scale must only reach several particle diameters to effectively reach this limit regardless of microscopic dynamics. For $\lambda \leq 3$, however, the MD and BD do not generally exhibit qualitatively similar curvature: for $\lambda = 3.0$ and 2.5, the BD curves show appreciable variation in diffusivity, while the MD curves are virtually flat; and for $\lambda = 2.0$ and 1.0, the BD and MD curves have opposite slopes (negative and positive, respectively).

Perhaps this lack of consistent correlation between local structure and dynamics arises because $\rho(z)$ is "too local" to be an adequate measure of the particles' structural environments. We address this in the right panel of Figure 3, where we plot the same diffusivity data against local packing fraction $\phi(z)$, which for HS contains a greater amount of information about the nature of particle packing than $\rho(z)$. While the data for both MD and BD do modestly collapse around their respective D_ϕ^{bulk} versus ϕ curves, $\phi(z)$ is clearly not a qualitatively strong predictor of local mobility for these systems. In fact, this transformation arises rather trivially because $\phi(z)$ itself collapses as a function of $\rho(z)$ as $\lambda \to 0$ (bottom inset). Given such a straightforward relationship between $\phi(z)$ and $\rho(z)$, it is unsurprising that packing fraction does not reconcile MD and BD behaviors with respect to λ.

In Figure 4, we consider correlations between local diffusivity and a more microscopic static property: the local available space $\exp\{c^{(1)}(z)\}$, which quantifies the fractional volume at z into which an additional HS particle can be inserted without overlap. (Note that $\exp\{c^{(1)}(z)\}$ is not simply equivalent to the void space defined by $\phi_{void}(z) = 1 - \phi(z)$.) Average available volume positively correlates with average diffusivity in the isotropic directions of bulk and inhomogeneous HS fluids more strongly than density or packing fraction,[45] making it a natural

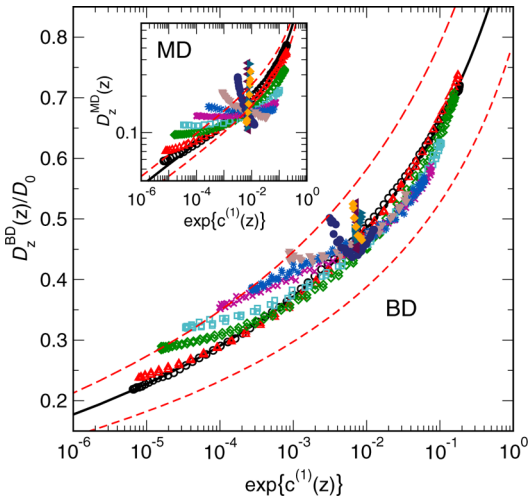

Figure 4. Position-dependent diffusivities in the inhomogeneous z-direction $D_z^{BD}(z)$ and $D_z^{MD}(z)$ (inset) plotted vs fractional available space $\exp\{c^{(1)}(z)\}$ for HS at $\rho_{avg} = 0.573$, $\rho(z) = [0.287, 0.860]$, and $\lambda = 24$, 12, 6, 4, 3, 2.5, 2.0, 1.5, 1.2, 1.1, and 1.0 (symbols consistent with Figure 3). Error bars are on the order of the scale of the symbols. Data for the bulk HS fluid are shown as solid lines and ±20% bounds on the bulk curves are plotted as dashed red lines. MD data are from a previous study by the authors.[57]

quantity to examine on a position-dependent basis. Additionally, it is known that average and local measures of available volume provide very similar information compared to excess entropy,[45,57] a thermodynamic property that is more generalizable (i.e., applicable to non-HS fluids) and well-known to semiquantitatively predict appropriately nondimensionalized transport coefficients for a wide array of fluid systems.[24−50]

Significantly, we observe that the $D_z^{BD}(z)$ curves at various λ roughly collapse onto a single curve as a function of $\exp\{c^{(1)}(z)\}$, at least relative to the $D_z^{MD}(z)$ curves, which exhibit highly nontrivial λ-dependent behaviors, including broadly positive (e.g., $\lambda = 12$), negative (e.g., $\lambda = 2$), and completely decoupled (e.g., $\lambda = 2.5,1.0$) correlations with $\exp\{c^{(1)}(z)\}$. For example, consider the wavelengths $\lambda \leq 1.5$:

dx.doi.org/10.1021/jp508887r | J. Phys. Chem. B XXXX, XXX, XXX−XXX

$D_z^{BD}(z)$ values show some curvature relative to $\exp\{c^{(1)}(z)\}$ (particularly at $\lambda = 1.5$), but overall deviate no more than ≈20% from the bulk reference curve (see dashed red lines in Figure 4); in contrast, the corresponding MD curves collapse very poorly, with $D_z^{MD}(z)$ varying by factors of about 3 when $\lambda = 1$, despite the fact that $\exp\{c^{(1)}(z)\}$ is virtually homogeneous at these wavelengths. This dichotomy in data collapse reinforces the idea that static-dynamics correlations for isotropic fluids do not necessarily generalize to describe particle mobility in inhomogeneous fluids, and furthermore that the quality of mapping between bulk and local behaviors is sensitive to the governing microscopic dynamics.

We conclude our discussion of local dynamics by examining whether the poor qualitative mapping between $D_z^{BD}(z)$ and $D_z^{MD}(z)$ might be corrected by using alternative diffusivity scalings already known to relate bulk transport coefficients from BD and MD simulations. The scalings we consider derive from fluids interacting via inverse power law (IPL) pair potentials, that is, $\varphi(r) = \varepsilon(\sigma/r)^{\mu}$, which are a reference model for dense fluids dominated by interparticle repulsions. For IPL fluids, it has been shown that there exists a one-to-one mapping between appropriately reduced (i.e., nondimensionalized) long-time bulk diffusivities from MD and BD.[24−26,63] These diffusivities are $\tilde{D}_\rho^{MD} = D_\rho^{MD}\rho^{1/3}(m/k_BT)^{1/2}$ (where $\rho^{1/3}$ corresponds to the mean interparticle spacing) and D_ρ^{BD}/D_0, respectively. Additionally, a heuristic function[64] based on the leading order dependencies of D_ρ^{BD} and D_ρ^{MD} upon density has been shown to quantitatively relate these quantities, given by

$$1 - D_\rho^{BD}/D_0 = \{1 + c_1\tilde{D}_\rho^{MD} + c_2(\tilde{D}_\rho^{MD})^{3/2}\}^{-1} \quad (6)$$

where c_1 and c_2 are constants. Equation 6 acts as a universal curve correlating $\tilde{D}_\rho^{MD}$ and D_ρ^{BD}/D_0 over a wide range of bulk state points not only for "hard" IPL fluids but also for diverse "soft" model fluids that exhibit complex diffusivity trends.[64,66] For our purposes, these nondimensional scalings represent an important test because IPL fluids with sufficient sharpness (i.e., $\mu \geq 48$) behave quite similarly to the HS system with respect to structure and long-time relaxation for the density range considered here.[63,82]

Does this one-to-one mapping between BD and MD transport coefficients generally apply to the local diffusivities of inhomogeneous fluids? To address this question, one necessary task is to identify an appropriate mean interparticle spacing to use when nondimensionalizing $\tilde{D}_z^{MD}(z)$. Using ρ_{avg} (as in the bulk) would only trivially shift all of the $\tilde{D}_z^{MD}(z)$ values considered thus far regardless of λ, since we have kept ρ_{avg} constant. However, it is evident from Figures 2−4 that λ affects the qualitative correspondence between BD and MD. A straightforward way to capture the influence of λ is to use local density $\rho(z)$. In Figure 5, we plot $D_z^{MD}(z)$ scaled by $\rho(z)$ versus the appropriately reduced $D_z^{BD}(z)$ values. (We also tested the more coarse-grained van der Waals and Tarazona weighted densities $\rho^{r}(z)$, which arise in density functional theory (DFT) for inhomogeneous fluids,[73,83] but these result in very similar curves.) Of course, for large wavelengths where $D_z^{BD}(z)$ and $D_z^{MD}(z)$ converge to locally "bulk-like" values (e.g., $\lambda \geq 12$), and the $\tilde{D}_z^{MD}(z)$ versus $1 - D^{BD}/D_0$ curves follow the form of eq 6; however, at smaller wavelengths (e.g., $\lambda \leq 6$), the bulk relationship between MD and BD diffusivities clearly breaks down. Given that the mapping between $\tilde{D}^{MD}$ and D^{BD}/D_0 is rigorous for repulsive model fluids,[24,26] this breakdown confirms, perhaps even more so than the previous plots, that bulk-derived connections between BD and MD transport coefficients demand scrutiny in the context of inhomogeneous particle mobility.

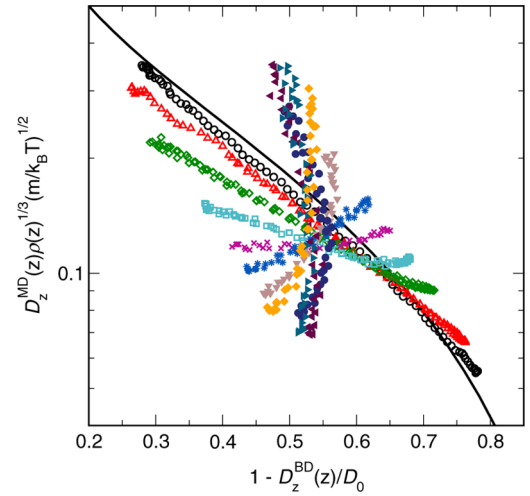

Figure 5. Nondimensionalized position-dependent diffusivities in the inhomogeneous z-direction in MD simulations $\tilde{D}^{MD}$ vs the fractional slowdown in BD diffusivity relative to the dilute limit, $1 - D_z^{BD}(z)/D_0$. The density used to scale $\tilde{D}^{MD}$ is local density $\rho(z)$. Curves are for HS systems at $\rho_{avg} = 0.573$, $\rho(z) = [0.287, 0.860]$, and $\lambda = 24$, 12, 6, 4, 3, 2.5, 2, 1.5, 1.2, 1.1, and 1.0 (symbols consistent with Figure 3). Error bars are on the scale of the symbols. The bulk relationship is shown as a solid black line. MD data are from a previous study by the authors.[57]

Average Dynamics of Inhomogeneous Fluids. In the top panel of Figure 6, we examine the λ-dependence of

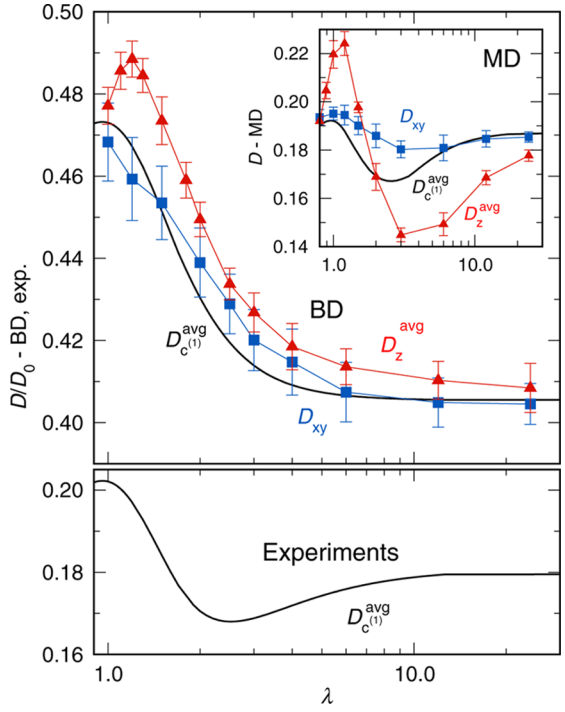

Figure 6. Average diffusivities D_z^{avg} (red triangles) and D_{xy} (blue squares) vs wavelength λ for HS fluids at $\rho_{avg} = 0.573$ and $\rho(z) = [0.287,0.860]$. Solid black lines are model predictions $D_{c^{(1)}}^{avg}$ from eq 8 (see discussion in text). The model prediction in the bottom panel draws upon experimental data collected for a variety of pseudo-HS colloids.[84] MD data are from a previous study by the authors.[57]

dx.doi.org/10.1021/jp508887r | J. Phys. Chem. B XXXX, XXX, XXX−XXX

measured average diffusivities D_z^{avg} and D_{xy}, which characterize some aspects of global single-particle mobility, and compare them with analytically derived "model" predictions of diffusivity for both BD and MD systems. Average diffusivity in the inhomogeneous direction is defined as[85]

$$D_z^{avg} = \int_0^{\lambda/2} D_z(z)\rho(z)dz / \int_0^{\lambda/2} \rho(z)dz \quad (7)$$

which results from the fact that D_z^{avg} is the average of the diffusivities of individual particles that are distributed according to $\rho(z)$.

For a given choice of microscopic dynamics, the measured D_z^{avg} and D_{xy} curves are roughly coupled as a function of λ, but the pairs of curves exhibit qualitatively distinct λ-dependencies for BD versus MD. Namely, the average BD diffusivities overall decrease upon transitioning from short λ, where they converge to the D_ρ^{bulk} associated with ρ_{avg} as $\lambda \to 0$, to long λ, where they converge to a noticeably shifted analytical limit of eq 7 as $\lambda \to \infty$. In contrast, the MD curves exhibit global minima around $\lambda \simeq 3$ and the long-λ limit is only subtly shifted from the bulk limit. The magnitudes of D_z^{avg} are also less sensitive to λ for BD relative to MD, with diffusivity increasing by ≈15% versus ≈60% between $3.0 \geq \lambda \geq 1.0$, respectively. Interestingly, both the BD and MD curves both exhibit relative maxima at $\lambda \simeq 1$, which approximately corresponds to stacked "sheets" of particles, and recalls previous studies showing that strongly layered density profiles maximize HS particle mobility along slit-pores.[44] Taken altogether, however, the measured curves demonstrate that despite the imposition of identical inhomogeneous static structures, different global diffusive trends emerge depending on the choice of microscopic dynamics.

The predicted curves in Figure 6 are calculated using the expression

$$D_{c^{(1)}}^{avg} = \int_0^{\lambda/2} D_{c^{(1)}}^{bulk}[c^{(1)}(z)]\rho(z)dz / \int_0^{\lambda/2} \rho(z)dz \quad (8)$$

which involves averaging over local diffusivity predictions derived by substituting the λ-dependent $c^{(1)}(z)$ profiles into the bulk HS relationship between diffusivity and fractional available volume. This approach is based on the idea that diffusion can be conceptualized as particles probing unoccupied space in their vicinity,[45,52] and we previously showed that eq 8 was an approximate predictor of diffusivities for inhomogeneous MD systems.[57] Here, we find it is equally successful for BD, despite the qualitatively different behaviors of BD and MD with respect to λ: the model lines in both cases approximately capture all extremes and converge to the correct short- and long-λ limits. This suggests that the underlying physics connecting structure and diffusivity in the bulk, while not necessarily directly applicable to local particle motions (see Figure 4), nonetheless play a more subtle role in driving global diffusion regardless of the type of governing microscopic dynamics. With this in mind, the differences between the predicted (and measured) diffusivity curves for BD and MD must emerge due to the different correlations between dynamics and available volume in the respective bulk fluids, where correlations are considerably stronger for MD than BD due to solvent friction effects in the latter. These stronger local correlations between static environment and dynamics in MD subsequently give rise to the prominent minimum in diffusivity at $\lambda \simeq 3$, which apparently presents a dynamically inefficient distribution of available volume. In contrast, the frictional effects in the BD system wash out this effect and hence eliminate the minimum.

Given that the BD and MD systems exhibit qualitatively different average diffusivities (via both measurement and prediction), a natural issue to consider is what these curves might look like for similar experimental systems, that is, pseudo-HS Brownian suspensions that are intrinsically subject to interparticle hydrodynamic interactions. We address this issue in the bottom panel of Figure 6, where we plot $D_{c^{(1)}}^{avg}$ predicted with eq 8 using a $D_{c^{(1)}}^{bulk}$ curve fit to self-diffusivity data collected for a variety of pseudo-HS colloids.[84] Interestingly, the predicted curve for the experimental systems has a different qualitative shape than the corresponding overdamped BD curves and is instead more similar to the MD curves, exhibiting a prominent minima at $\lambda \simeq 3$. This is surprising given that BD might intuitively be considered a better approximation of experiments due to its incorporation of the stochastic movements characteristic of real colloids. While it is beyond the scope of this study whether the model prediction for experiments is borne out by direct measurements, comparisons between all three of the $D_{c^{(1)}}^{avg}$ curves demonstrate that one should be wary of assuming that even the average transport coefficients of inhomogeneous fluids straightforwardly map between systems governed by different microscopic dynamics. Furthermore, these findings suggest that in order to approximate real colloidal physics, one might simply choose MD (rather than BD) if chiefly interested in efficiency, or alternatively use techniques that fully incorporate one-body inertia and many-body hydrodynamic interactions, for example, Stokesian dynamics.[86−88]

Drawing upon the predictive capability of eq 8, we can also rapidly survey a larger variety of $\rho(z)$ profiles, with not only diverse wavelengths λ, but also average densities ρ_{avg} and amplitudes A (recall eq 1). In the top panel of Figure 7, we examine the λ-dependence of $D_{c^{(1)}}^{avg}$ predictions for BD at several amplitudes A given an average density $\rho_{avg} = 0.6$ (comparable to $\rho_{avg} = 0.573$ in Figures 2−6). It is evident that the qualitative λ-dependence of the $D_{c^{(1)}}^{avg}$ curves is invariant with respect to A, where extrema in the functional form of $D_{c^{(1)}}^{avg}(\lambda|A)$ simply become more exaggerated as A increases. In other words, average particle mobility becomes increasingly sensitive to wavelength as the density variations increase in scale. The form of $D_{c^{(1)}}^{avg}(\lambda)$ also remains the same for fluids with $0.2 \leq \rho_{avg} \leq 0.8$ and appropriate ranges of A. (Note that any choice of A must necessarily avoid accessing $\rho(z) \leq 0$ or any $\rho(z)$ large enough that the functional relationship between $D_{c^{(1)}}^{bulk}$ and $c^{(1)}$ would break down.) Similar findings apply for the analogous families of curves as calculated for MD and experimental systems, though naturally the respective functional forms of $D_{c^{(1)}}^{avg}(\lambda)$ resemble those in Figure 6.

As a closing consideration, we compare the top and bottom panels in Figure 7 to demonstrate a subtle but important point regarding the connection between available space and particle mobility: while $\exp\{c^{(1)}(z)\}$ profiles can be used via eq 8 to approximately predict diffusivity, this is not indicative of a broader positive correlation between average diffusivity and average available space. In other words, simply perturbing fluid structure to generate relatively more available space on average does not necessarily result in relatively faster relaxation processes. The bottom panel of Figure 7 shows the average fraction of available space as defined by

dx.doi.org/10.1021/jp508887r | J. Phys. Chem. B XXXX, XXX, XXX−XXX

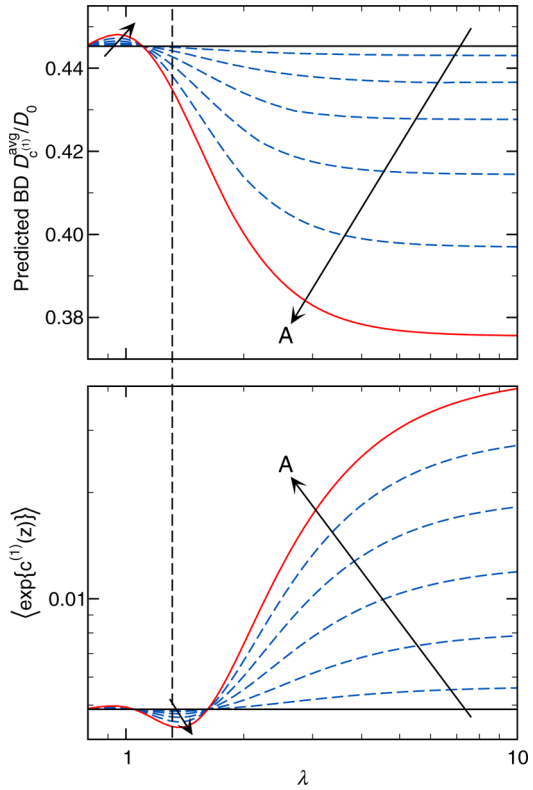

Figure 7. $D_{c^{(1)}}^{avg}$ (top) and average available space $\langle \exp\{c^{(1)}(z)\}\rangle$ (bottom) vs λ for BD HS systems with $\rho(z)$ profiles defined by ρ_{avg} = 0.6 and amplitudes A = 0.0, 0.1, 0.2, 0.3, 0.4, 0.5, and 0.6 (see eq 1). The solid black line (A = 0.0) corresponds to the bulk fluid and the red line (A = 0.6) represents the series of systems most similar to those analyzed in Figures 2−6 (i.e., ρ_{avg} = 0.573, A = 0.573). See text for discussion of the vertical dashed line.

$$\langle \exp\{c^{(1)}(z)\}\rangle = (2/\lambda)\int_0^{\lambda/2} \exp\{c^{(1)}(z)\}\mathrm{d}z \tag{9}$$

for the λ, A, and ρ_{avg} values presented in the top panel. It is evident that the most available space on average emerges upon imposition of long-wavelength density variations. This is due to the imposition of wide regions of relatively low density, combined with the bulk-like negative logarithmic correlation between $\exp\{c^{(1)}(z)\}$ and $\rho(z)$ at long λ. However, as seen in the top panel of Figure 7, this same limit coincides with global minima in average diffusivity because particles must also traverse equally wide regions of high density where diffusivity slows down (regions that are more important from a "mass flux" perspective; see eq 7).

While this means there is no general positive correlation between diffusivity and available space, we do note that these quantities are roughly positively correlated below $\lambda \leq 1.2$, marked in Figure 7 by a vertical dashed line. Most studies examining static-dynamic correlations for inhomogeneous fluids have focused on this regime (i.e., $\lambda \simeq 1$), hence, the previous success in using available volume (or, equivalently, excess entropy) to predict average transport coefficients.[45] But for $\exp\{c^{(1)}(z)\}$ profiles to be useful as general predictors of diffusivity for inhomogeneous fluids, we find they should be used in the context of eq 8, which requires an accurate functional relationship between bulk diffusivity and available volume.

CONCLUSIONS

Unlike the simple scalable relationships that link the transport coefficients of bulk isotropic fluids treated governed by Brownian versus Newtonian mechanics, the results presented here demonstrate that local and global single-particle mobilities of inhomogeneous fluids are qualitatively sensitive to the type of governing microscopic dynamics. As we show, when available volume and particle density exhibit strong inhomogeneities in a fluid, differences between how mobility correlates to density due to the microscopic dynamics (reflected even in the bulk fluid) should be expected to produce a nontrivial relationship between average transport properties of inhomogeneous fluids treated by MD and BD that depends on the details of the density profile. Moreover, for even the simple systems considered here, correlations between local diffusivity and static structure nontrivially depend upon inhomogeneity wavelength, and for wavelengths below several particle diameters, these correlations are distinct for BD and MD. Accordingly, it is problematic to identify a physically intuitive local static quantity (i.e., a "mechanistic" description) that universally predicts both isotropic (e.g., bulk) and position-dependent mobility for these systems, and existing functional one-to-one relationships between BD and MD transport coefficients, valid for bulk systems with diverse interaction potentials, do not apply to position-dependent particle motions in strongly inhomogeneous fluids.

An overarching goal of this study was to compare two types of physics normally associated with "colloidal" and "atomic" fluid regimes, as exemplified by BD and MD, respectively, but our findings suggest that these designations might be problematic. This originates from our discovery of a simple expression (eq 8) that predicts the dependence of average particle mobility upon static structure via information about available space and bulk diffusivity. A highlight here is that the expression is successful for both BD and MD, capturing the qualitative dichotomies that emerge between their respective diffusivities as a function of inhomogeneity wavelength. More crucially, similar predictions for experimental pseudo-HS colloids qualitatively differ with BD (i.e., overdamped Langevin) simulations, with MD results instead better reflecting the behaviors expected from the experimental systems. Thus, if one is interested in studying the dynamics of strongly inhomogeneous colloidal suspensions via computer simulations, these results not only recommend MD over BD treated at the simplest level, but also emphasize the need for further comparisons with more sophisticated techniques incorporating effects due to inertia and hydrodynamic interactions.[86−88]

Looking beyond the simple inhomogeneous fluids considered here, it would be fruitful to examine the dynamic behaviors that emerge in more complex systems, such as those with soft or multilength scale interparticle potentials, or those where dynamic heterogeneity is imposed not by static external fields, but instead by nonequilibrium sources such as shear forces. Meanwhile, the one-to-one scaling relationships between bulk transport coefficients from BD and MD, which we find are not straightforwardly applicable to local mobility, might also be reconsidered via tests more closely aligned with the concepts of strongly correlating (i.e., "isomorphic") fluids, for which the bulk scalings can be directly derived.[26,27] Finally, this study highlights the need to reconsider which simulation techniques are truly most suitable in terms of modeling real colloidal dynamics, issues that might be addressed by tracking particle

dx.doi.org/10.1021/jp508887r | J. Phys. Chem. B XXXX, XXX, XXX−XXX

motions in experimental systems[89] and several simulated approximations in tandem, a line of inquiry that we will report upon in future publications.

■ ASSOCIATED CONTENT

Supporting Information

Depths of external oscillatory potentials $\varphi^{osc}(z)$ versus wavelength λ. This material is available free of charge via the Internet at http://pubs.acs.org.

■ AUTHOR INFORMATION

Corresponding Author

*E-mail: truskett@che.utexas.edu.

Notes

The authors declare no competing financial interest.

■ ACKNOWLEDGMENTS

This work was supported by the Gulf of Mexico Research Initiative, the Robert A. Welch Foundation (F-1696), and the National Science Foundation (CBET-1403768). We also acknowledge the Texas Advanced Computing Center (TACC) at The University of Texas at Austin for providing HPC resources for this study.

■ REFERENCES

(1) Perrin, J. Brownian Motion and Molecules. *J. Phys. (Paris)* **1910**, *9*, 5−39.
(2) Biben, T.; Hansen, J.; Barrat, J. Density Profiles of Concentrated Colloidal Suspensions in Sedimentation Equilibrium. *J. Chem. Phys.* **1993**, *98*, 7330−7344.
(3) van Blaaderen, A.; Ruel, R.; Wiltzius, P. Template-Directed Colloidal Crystallization. *Nature* **1997**, *385*, 321−324.
(4) Royall, C. P.; van Roij, R.; van Blaaderen, A. Extended Sedimentation Profiles in Charged Colloids: The Gravitational Length, Entropy, and Electrostatics. *J. Phys.: Condens. Matter* **2005**, *17*, 2315−2326.
(5) Lin, K.; Crocker, J. C.; Prasad, V.; Schofield, A.; Weitz, D. A.; Lubensky, T. C.; Yodh, A. G. Entropically Driven Colloidal Crystallization on Patterned Surfaces. *Phys. Rev. Lett.* **2000**, *85*, 1770−1773.
(6) Bahukudumbi, P.; Bevan, M. A. Imaging Energy Landscapes with Concentrated Diffusing Colloidal Probes. *J. Chem. Phys.* **2007**, *126*, 244702.
(7) Sullivan, M. T.; Zhao, K.; Hollingsworth, A. D.; Austin, R. H.; Russel, W. B.; Chaikin, P. M. An Electric Bottle for Colloids. *Phys. Rev. Lett.* **2006**, *96*, 015703.
(8) Juárez, J. J.; Bevan, M. A. Interactions and Microstructures in Electric Field Mediated Colloidal Assembly. *J. Chem. Phys.* **2009**, *131*, 134704.
(9) Grier, D. G. A Revolution in Optical Manipulation. *Nature* **2003**, *424*, 810−816.
(10) Jamie, E. A. G.; Wensink, H. H.; Aarts, D. G. A. L. Probing the Critical Behavior of Colloidal Interfaces by Gravity. *Soft Matter* **2010**, *6*, 250−255.
(11) Israelachvili, J. N. *Intermolecular and Surface Forces*; Academic Press: New York, NY, U.S.A., 2011.
(12) Williams, I.; Oğuz, E. C.; Bartlett, P.; Löwen, H.; Royall, C. P. Direct Measurement of Osmotic Pressure via Adaptive Confinement of Quasi Hard Disc Colloids. *Nat. Commun.* **2013**, *4*, 1−6.
(13) Wu, J.; Li, Z. Density-Functional Theory for Complex Fluids. *Annu. Rev. Phys. Chem.* **2007**, *58*, 85−112.
(14) Roth, R. Fundamental Measure Theory for Hard-Sphere Mixtures: A Review. *J. Phys.: Condens. Matter* **2010**, *22*, 063102.
(15) Krakoviack, V. Liquid−Glass Transition of Confined Fluids: Insights from a Mode-Coupling Theory. *J. Phys.: Condens. Matter* **2005**, *17*, S3565.
(16) Biroli, G.; Bouchaud, J.-P.; Miyazaki, K.; Reichman, D. R. Inhomogeneous Mode-Coupling Theory and Growing Dynamic Length in Supercooled Liquids. *Phys. Rev. Lett.* **2006**, *97*, 195701.
(17) Archer, A. J. Dynamical Density Functional Theory for Dense Atomic Liquids. *J. Phys.: Condens. Matter* **2006**, *18*, 5617.
(18) Krakoviack, V. Mode-Coupling Theory for the Slow Collective Dynamics of Fluids Adsorbed in Disordered Porous Media. *Phys. Rev. E* **2007**, *75*, 031503.
(19) Lang, S.; Boţan, V.; Oettel, M.; Hajnal, D.; Franosch, T.; Schilling, R. Glass Transition in Confined Geometry. *Phys. Rev. Lett.* **2010**, *105*, 125701.
(20) Lang, S.; Schilling, R.; Krakoviack, V.; Franosch, T. Mode-Coupling Theory of the Glass Transition for Confined Fluids. *Phys. Rev. E* **2012**, *86*, 021502.
(21) Becker, T.; Nelissen, K.; Cleuren, B.; Partoens, B.; Van den Broeck, C. Diffusion of Interacting Particles in Discrete Geometries. *Phys. Rev. Lett.* **2013**, *111*, 110601.
(22) Lang, S.; Franosch, T. Tagged-Particle Motion in a Dense Confined Liquid. *Phys. Rev. E* **2014**, *89*, 062122.
(23) Jain, A.; Bollinger, J. A.; Truskett, T. M. Inverse Methods for Material Design. *AIChE J.* **2014**, *60*, 2732−2740.
(24) Rosenfeld, Y. Relation Between the Transport Coefficients and the Internal Entropy of Simple Systems. *Phys. Rev. A* **1977**, *15*, 2545−2549.
(25) Rosenfeld, Y. A Quasi-Universal Scaling Law for Atomic Transport in Simple Fluids. *J. Phys.: Condens. Matter* **1999**, *11*, 5415.
(26) Gnan, N.; Schrøder, T. B.; Pedersen, U. R.; Bailey, N. P.; Dyre, J. C. Pressure-Energy Correlations in Liquids. IV. "Isomorphs" in Liquid Phase Diagrams. *J. Chem. Phys.* **2009**, *131*, 234504.
(27) Dyre, J. C. Hidden Scale Invariance in Condensed Matter. *J. Phys. Chem. B* **2014**, *118*, 10007−10024.
(28) Dzugutov, M. A Universal Scaling Law for Atomic Diffusion in Condensed Matter. *Nature* **1996**, *381*, 137−139.
(29) Hoyt, J. J.; Asta, M.; Sadigh, B. Test of the Universal Scaling Law for the Diffusion Coefficient in Liquid Metals. *Phys. Rev. Lett.* **2000**, *85*, 594−597.
(30) Li, G. X.; Liu, C. S.; Zhu, Z. G. Scaling Law for Diffusion Coefficients in Simple Melts. *Phys. Rev. B* **2005**, *71*, 094209.
(31) Sharma, R.; Chakraborty, S. N.; Chakravarty, C. Entropy, Diffusivity, and Structural Order in Liquids with Waterlike Anomalies. *J. Chem. Phys.* **2006**, *125*, 204501.
(32) Mittal, J.; Errington, J. R.; Truskett, T. M. Quantitative Link between Single-Particle Dynamics and Static Structure of Supercooled Liquids. *J. Phys. Chem. B* **2006**, *110*, 18147−18150.
(33) Mittal, J.; Errington, J. R.; Truskett, T. M. Relationship between Thermodynamics and Dynamics of Supercooled Liquids. *J. Chem. Phys.* **2006**, *125*, 076102.
(34) Errington, J. R.; Truskett, T. M.; Mittal, J. Excess-Entropy-Based Anomalies for a Waterlike Fluid. *J. Chem. Phys.* **2006**, *125*, 244502.
(35) (a) Abramson, E. H.; West-Foyle, H. Viscosity of Nitrogen Measured to Pressures of 7 GPa and Temperatures of 573 K. *Phys. Rev. E* **2008**, *77*, 041202. (b) Abramson, E. H. Viscosity of Carbon Dioxide Measured to a Pressure of 8 GPa and Temperature of 673 K. *Phys. Rev. E* **2009**, *80*, 021201. (c) Abramson, E. H. Viscosity of Argon to 5 GPa and 673 K. *High Pressure Res.* **2011**, *31*, 544−548. (d) Abramson, E. H. Viscosity of Methane to 6 GPa and 673 K. *Phys. Rev. E* **2011**, *84*, 062201.
(36) Krekelberg, W. P.; Pond, M. J.; Goel, G.; Shen, V. K.; Errington, J. R.; Truskett, T. M. Generalized Rosenfeld Scalings for Tracer Diffusivities in Not-So-Simple Fluids: Mixtures and Soft Particles. *Phys. Rev. E* **2009**, *80*, 061205.
(37) Chopra, R.; Truskett, T. M.; Errington, J. R. On the Use of Excess Entropy Scaling to Describe the Dynamic Properties of Water. *J. Phys. Chem. B* **2010**, *114*, 10558−10566.
(38) Pond, M. J.; Errington, J. R.; Truskett, T. M. Communication: Generalizing Rosenfeld's Excess-Entropy Scaling to Predict Long-Time Diffusivity in Dense Fluids of Brownian Particles: From Hard to Ultrasoft Interactions. *J. Chem. Phys.* **2011**, *134*, 081101.

(39) Ingebrigtsen, T. S.; Schrøder, T. B.; Dyre, J. C. What Is a Simple Liquid? *Phys. Rev. X* **2012**, *2*, 011011.
(40) Nayar, D.; Chakravarty, C. Water and Water-Like Liquids: Relationships between Structure, Entropy and Mobility. *Phys. Chem. Chem. Phys.* **2013**, *15*, 14162−14177.
(41) Mittal, J.; Errington, J. R.; Truskett, T. M. Thermodynamics Predicts How Confinement Modifies the Dynamics of the Equilibrium Hard-Sphere Fluid. *Phys. Rev. Lett.* **2006**, *96*, 177804.
(42) Mittal, J.; Errington, J. R.; Truskett, T. M. Relationships between Self-Diffusivity, Packing Fraction, and Excess Entropy in Simple Bulk and Confined Fluids. *J. Phys. Chem. B* **2007**, *111*, 10054−10063.
(43) Mittal, J.; Shen, V. K.; Errington, J. R.; Truskett, T. M. Confinement, Entropy, and Single-Particle Dynamics of Equilibrium Hard-Sphere Mixtures. *J. Chem. Phys.* **2007**, *127*, 154513.
(44) Goel, G.; Krekelberg, W. P.; Errington, J. R.; Truskett, T. M. Tuning Density Profiles and Mobility of Inhomogeneous Fluids. *Phys. Rev. Lett.* **2008**, *100*, 106001.
(45) Goel, G.; Krekelberg, W. P.; Pond, M. J.; Mittal, J.; Shen, V. K.; Errington, J. R.; Truskett, T. M. Available States and Available Space: Static Properties That Predict Self-Diffusivity of Confined Fluids. *J. Stat. Mech.: Theory Exp.* **2009**, *2009*, P04006.
(46) Chopra, R.; Truskett, T. M.; Errington, J. R. Excess-Entropy Scaling of Dynamics for a Confined Fluid of Dumbbell-Shaped Particles. *Phys. Rev. E* **2010**, *82*, 041201.
(47) Borah, B. J.; Maiti, P. K.; Chakravarty, C.; Yashonath, S. Transport in Nanoporous Zeolites: Relationships between Sorbate Size, Entropy, and Diffusivity. *J. Chem. Phys.* **2012**, *136*, 174510.
(48) Ma, X.; Chen, W.; Wang, Z.; Peng, Y.; Han, Y.; Tong, P. Test of the Universal Scaling Law of Diffusion in Colloidal Monolayers. *Phys. Rev. Lett.* **2013**, *110*, 078302.
(49) Liu, Y.; Fu, J.; Wu, J. Excess-Entropy Scaling for Gas Diffusivity in Nanoporous Materials. *Langmuir* **2013**, *29*, 12997−13002.
(50) Ingebrigtsen, T. S.; Errington, J. R.; Truskett, T. M.; Dyre, J. C. Predicting How Nanoconfinement Changes the Relaxation Time of a Supercooled Liquid. *Phys. Rev. Lett.* **2013**, *111*, 235901.
(51) Liu, P.; Harder, E.; Berne, B. J. On the Calculation of Diffusion Coefficients in Confined Fluids and Interfaces with an Application to the Liquid−Vapor Interface of Water. *J. Phys. Chem. B* **2004**, *108*, 6595−6602.
(52) Mittal, J.; Truskett, T. M.; Errington, J. R.; Hummer, G. Layering and Position-Dependent Diffusive Dynamics of Confined Fluids. *Phys. Rev. Lett.* **2008**, *100*, 145901.
(53) Sedlmeier, F.; Hansen, Y.; Mengyu, L.; Horinek, D.; Netz, R. Water Dynamics at Interfaces and Solutes: Disentangling Free Energy and Diffusivity Contributions. *J. Stat. Phys.* **2011**, *145*, 240−252.
(54) Mittal, J.; Hummer, G. Pair Diffusion, Hydrodynamic Interactions, and Available Volume in Dense Fluids. *J. Chem. Phys.* **2012**, *137*, 034110.
(55) Olivares-Rivas, W.; Colmenares, P. J.; López, F. Direct Evaluation of the Position Dependent Diffusion Coefficient and Persistence Time from the Equilibrium Density Profile in Anisotropic Fluids. *J. Chem. Phys.* **2013**, *139*, 074103.
(56) von Hansen, Y.; Gekle, S.; Netz, R. R. Anomalous Anisotropic Diffusion Dynamics of Hydration Water at Lipid Membranes. *Phys. Rev. Lett.* **2013**, *111*, 118103.
(57) Bollinger, J. A.; Jain, A.; Truskett, T. M. Structure, Thermodynamics, and Position-Dependent Diffusivity in Fluids with Sinusoidal Density Variations. *Langmuir* **2014**, *30*, 8247−8252.
(58) Carmer, J.; van Swol, F.; Truskett, T. M. Position-Dependent and Pair Diffusivity Profiles from Steady-State Solutions of Color Reaction-Counterdiffusion Problems. *J. Chem. Phys.* **2014**, *141*, 046101.
(59) Foffi, G.; Dawson, K. A.; Buldyrev, S. V.; Sciortino, F.; Zaccarelli, E.; Tartaglia, P. Evidence for an Unusual Dynamical-Arrest Scenario in Short-Ranged Colloidal Systems. *Phys. Rev. E* **2002**, *65*, 050802.
(60) Krekelberg, W. P.; Mittal, J.; Ganesan, V.; Truskett, T. M. How Short-Range Attractions Impact the Structural Order, Self-Diffusivity, and Viscosity of a Fluid. *J. Chem. Phys.* **2007**, *127*, 044502.
(61) Moreno, A. J.; Likos, C. N. Diffusion and Relaxation Dynamics in Cluster Crystals. *Phys. Rev. Lett.* **2007**, *99*, 107801.
(62) Berthier, L.; Moreno, A. J.; Szamel, G. Increasing the Density Melts Ultrasoft Colloidal Glasses. *Phys. Rev. E* **2010**, *82*, 060501.
(63) Lange, E.; Caballero, J. B.; Puertas, A. M.; Fuchs, M. Comparison of Structure and Transport Properties of Concentrated Hard and Soft Sphere Fluids. *J. Chem. Phys.* **2009**, *130*, 174903.
(64) Pond, M. J.; Errington, J. R.; Truskett, T. M. Mapping Between Long-Time Molecular and Brownian Dynamics. *Soft Matter* **2011**, *7*, 9859−9862.
(65) López-Flores, L.; Mendoza-Méndez, P.; Sánchez-Díaz, L. E.; Yeomans-Reyna, L. L.; Vizcarra-Rendón, A.; Pérez-Ángel, G.; Chávez-Páez, M.; Medina-Noyola, M. Dynamic Equivalence Between Atomic and Colloidal Liquids. *Europhys. Lett.* **2012**, *99*, 46001.
(66) Khrapak, S. A.; Vaulina, O. S.; Morfill, G. E. Self-Diffusion in Strongly Coupled Yukawa Systems (Complex Plasmas). *Phys. Plasmas* **2012**, *19*, 034503.
(67) López-Flores, L.; Ruíz-Estrada, H.; Chávez-Páez, M.; Medina-Noyola, M. Dynamic Equivalences in the Hard-Sphere Dynamic Universality Class. *Phys. Rev. E* **2013**, *88*, 042301.
(68) Löwen, H.; Hansen, J.-P.; Roux, J.-N. Brownian Dynamics and Kinetic Glass Transition in Colloidal Suspensions. *Phys. Rev. A* **1991**, *44*, 1169−1181.
(69) Gleim, T.; Kob, W.; Binder, K. How Does the Relaxation of a Supercooled Liquid Depend on Its Microscopic Dynamics? *Phys. Rev. Lett.* **1998**, *81*, 4404−4407.
(70) Szamel, G.; Flenner, E. Independence of the Relaxation of a Supercooled Fluid from Its Microscopic Dynamics: Need for Yet Another Extension of the Mode-Coupling Theory. *Europhys. Lett.* **2004**, *67*, 779.
(71) Berthier, L.; Kob, W. The Monte Carlo Dynamics of a Binary Lennard-Jones Glass-Forming Mixture. *J. Phys.: Condens. Matter* **2007**, *19*, 205130.
(72) (a) Berthier, L.; Biroli, G.; Bouchaud, J.-P.; Kob, W.; Miyazaki, K.; Reichman, D. R. Spontaneous and Induced Dynamic Fluctuations in Glass Formers. I. General Results and Dependence on Ensemble and Dynamics. *J. Chem. Phys.* **2007**, *126*, 184503. (b) Berthier, L.; Biroli, G.; Bouchaud, J.-P.; Kob, W.; Miyazaki, K.; Reichman, D. R. Spontaneous and Induced Dynamic Correlations in Glass Formers. II. Model Calculations and Comparison to Numerical Simulations. *J. Chem. Phys.* **2007**, *126*, 184504.
(73) Hansen, J.-P.; McDonald, I. R. *Theory of Simple Liquids*, 3rd ed.; Academic Press: New York, NY, U.S.A., 2006.
(74) Chandler, D.; Weeks, J. D.; Andersen, H. C. Van der Waals Picture of Liquids, Solids, and Phase Transformations. *Science* **1983**, *220*, 787−794.
(75) Hoang, H.; Galliero, G. Shear Viscosity of Inhomogeneous Fluids. *J. Chem. Phys.* **2012**, *136*, 124902.
(76) Dalton, B. A.; Glavatskiy, K. S.; Daivis, P. J.; Todd, B. D.; Snook, I. K. Linear and Nonlinear Density Response Functions for a Simple Atomic Fluid. *J. Chem. Phys.* **2013**, *139*, 044510.
(77) Weiss, G. H. *Adv. Chem. Phys.*; John Wiley & Sons, Inc.: New York, 2007; pp 1−18.
(78) Hinczewski, M.; von Hansen, Y.; Dzubiella, J.; Netz, R. R. How the Diffusivity Profile Reduces the Arbitrariness of Protein Folding Free Energies. *J. Chem. Phys.* **2010**, *132*, 245103.
(79) Hess, B.; Kutzner, C.; van der Spoel, D.; Lindahl, E. GROMACS 4: Algorithms for Highly Efficient, Load-Balanced, and Scalable Molecular Simulation. *J. Chem. Theory Comput.* **2008**, *4*, 435−447.
(80) Ermak, D. L.; McCammon, J. A. Brownian Dynamics with Hydrodynamic Interactions. *J. Chem. Phys.* **1978**, *69*, 1352−1360.
(81) Allen, M. P.; Tildesley, D. J. *Computer Simulation of Liquids*; Clarendon Press: New York, NY, U.S.A., 1989.
(82) Heyes, D. M.; Branka, A. C. The Influence of Potential Softness on the Transport Coefficients of Simple Fluids. *J. Chem. Phys.* **2005**, *122*, 234504.

(83) Davis, H. T. *Statistical Mechanics of Phases, Interfaces, and Thin Films*; Wiley-VCH: New York, NY, U.S.A., 1996.
(84) Lionberger, R. A.; Russel, W. B. A Smoluchowski Theory with Simple Approximations for Hydrodynamic Interactions in Concentrated Dispersions. *J. Rheol.* **1997**, *41*, 399−425.
(85) Bitsanis, I.; Magda, J. J.; Tirrell, M.; Davis, H. T. Molecular Dynamics of Flow in Micropores. *J. Chem. Phys.* **1987**, *87*, 1733−1750.
(86) Durlofsky, L.; Brady, J. F.; Bossis, G. Dynamic Simulation of Hydrodynamically Interacting Particles. *J. Fluid Mech.* **1987**, *180*, 21−49.
(87) Brady, J. F.; Bossis, G. Stokesian Dynamics. *Annu. Rev. Fluid Mech.* **1988**, *20*, 111−157.
(88) Sierou, A.; Brady, J. F. Accelerated Stokesian Dynamics Simulations. *J. Fluid Mech.* **2001**, *448*, 115−146.
(89) Weeks, E. R.; Crocker, J. C.; Levitt, A. C.; Schofield, A.; Weitz, D. A. Three-Dimensional Direct Imaging of Structural Relaxation Near the Colloidal Glass Transition. *Science* **2000**, *287*, 627−631.

dx.doi.org/10.1021/jp508887r | *J. Phys. Chem. B* XXXX, XXX, XXX−XXX